Spectral mixture analysis for subpixel classification of coconut

C. Palaniswami*, A. K. Upadhyay and H. P. Maheswarappa

Central Plantation Crops Research Institute, Kasaragod 671 124, India

The present study was undertaken to test the stability of a spectral mixture modelling method by applying the model to produce land-cover maps of coconut in Kasaragod district, Kerala. Classification results from applying the Spectral Mixture Analysis (SMA) were assessed by comparison with ground-truth data. SMA was performed and evaluated based on Landsat-7 ETM$^+$ (Enhanced Thematic Mapper Plus) data. Landsat-7 ETM$^+$ was available at 30 m resolution with six spectral bands (excluding the panchromatic band and thermal band). The Landsat-7 ETM$^+$ scene used in this study was acquired on 8 August 2000 from path 135, row 21. The scene was a level-2 product and was radiometrically and geometrically corrected (systematic) and resampled to give 25 m resolution. The commercial image processing software, IDRISI32 was used here for data visualization. The procedure used in this study was based on a linear mixture model to derive continuous fields of coconut, road, laterite outcrops, construction, arecanut and cloud. SMA was done on DN values and corresponding radiance values of the satellite imagery. The accuracy of endmember fraction was estimated as the mean of the percentage absolute difference between actual and modelled estimates. The subpixel accuracy achieved for the coconut land-cover was 87% using SMA of DN values, while it was 93% for SMA of radiance values.

Keywords: Coconut, remote sensing, spectral mixture analysis, subpixel classification.

IN general, remote sensing provides important coverage, mapping and classification of land-cover features, such as vegetation, soil, water and forests. A chief use of remotely sensed data is to produce a classification map of the identifiable or meaningful features or classes of land-cover types in a scene[1]. As a result, the chief product is a thematic map with themes such as land use, geology and vegetation types. In the field of remote sensing, image classification is a process in which pixels or the basic units of an image are assigned to classes. By comparing pixels to one another and to those of known identity, it is possible to assemble groups of similar pixels into classes that match the informational categories of interest to users of remotely sensed data. Numerous methods of image classification exist and classification has formed an important part of not only remote sensing, but also of the fields of image analysis and pattern recognition. In some instances, the classification itself may form the object of the analysis and serve as the final product. In other instances, the classification may form only an intermediate step in more elaborate analyses, such as land-degradation studies, process studies, landscape modelling, coastal zone management, resource management and other environment-monitoring applications. Therefore, image classification forms an important tool for examining digital images. Accordingly, the selection of which classification technique to employ can have substantial effect on the results of whether the classification is used as a final product or as one of several analytical procedures applied to derive information from an image for further analyses.

Image classification is defined as the process of creating thematic maps from satellite imagery[2]. Extraction of thematic information from remotely sensed images into the form of a thematic map is a key area of research into the applications of remote-sensing data. By definition, a thematic map is an informational representation of an image, which conveys information regarding the spatial distribution of a particular theme[3]. Themes may be as diversified as their areas of interest. Examples of themes include soil, vegetation, water depth and atmosphere. The objective of image classification is to classify each pixel of an image into land-cover categories. In the case of crisp or hard classification, each pixel is assigned to only one class. However, in fuzzy or soft classification, a pixel is associated with many land-cover classes. In general, classification techniques may be categorized by the training process on which they are based (supervized or unsupervized) or on the basis of the underlying theoretical model (parametric or non-parametric). The term classifier refers loosely to a computer program that implements a specific procedure for image classification. Many classification strategies have been devised over the years and from these alternatives, the analyst must select the classifier that will best serve the task or application at hand. The optimal classifier depends on the situation at hand since characteristics of each image and the circumstances for each study vary greatly. Therefore, it is imperative that the spatial analyst understands the alternative strategies available for image classification in order to select the most appropriate classifier for a specific task.

An alternative approach is to use a mixed pixel method or spectral mixture analysis (SMA). This method recognizes that a single pixel is typically made up of a number of varied spectral types (i.e. soil, water, vegetation)[4,5]. In effect, SMA is a technique used to measure the percentage of spectra for each land-cover type in a single pixel. In previous studies, SMA has been successfully used to classify successional forest types and forest types of varying carbon-sink strengths[6]. The SMA process enables the classification of different forest types, although it still has difficulties in classifying species type and age class with confidence. Using ground-based data is especially

*For correspondence. (e-mail: darsanpalaniswami@yahoo.co.uk)

useful with respect to increasing the accuracy of such classifications.

SMA is based on the assumption that the reflectance spectrum derived from an air- or space-borne sensor can be deconvolved into a linear mixture of the spectra of different ground components, frequently referred to as spectral endmembers[7]. Various methods of SMA have been developed to improve the classification of mixed pixels and to detect and identify subpixel components and their proportions. Most of the techniques have employed a linear mixing approach[8,9]. Linear mixing refers to additive combinations of several diverse materials that occur in patterns too fine to be resolved by the sensors.

The objective of this study was to test the stability of a spectral mixture modelling method by applying the model to produce land-cover maps of coconut in the study area. Classification results from applying the spectral mixture model were assessed by comparison with ground-truth data. The SMA was performed and evaluated based on Landsat-7 ETM$^+$ data.

The study area is part of Kasaragod district, Kerala. Landsat-7 ETM$^+$ was available at 30 m resolution with six spectral bands (excluding the panchromatic band and thermal band) (1: 0.45–0.52 μm; 2: 0.53–0.61 μm; 3: 0.63–0.69 μm; 4: 0.78–0.90 μm; 5: 1.55–1.75 μm; 7: 2.09–2.35 μm). The Landsat-7 ETM$^+$ scene used in this study was acquired on 8 August 2000 from path 135, row 21. The scene was a level-2 product and was radiometrically and geometrically corrected (systematic) and resampled to give 25 m resolution of Survey of India toposheet number 48L/15 and 48P/3. The resulting product is free from distortions related to the sensor (e.g. jitter, view-angle effect), satellite (e.g. attitude deviations from nominal), and earth (e.g. rotation, curvature).

The linear mixture model assumes that as long as the radiation from component patches remains separate until it reaches the sensor, it is possible to estimate proportions of component surfaces from the observed pixel brightness.

In effect, with a known number of endmembers and known spectra of each pure component, the observed pixel value in any spectral band is modelled by a linear combination of the spectral response of a component within the pixel.

The linear mixture model was applied with six endmembers or continuous fields to be estimated for each pixel of a six-band Landsat image; the mixture model becomes:

$$\mathrm{DN} = (R_{a1} \times F_a) + (R_{b1} \times F_b) + (R_{c1} \times F_c) + (R_{d1} \times F_d) + (R_{e1} \times F_e) + (R_{f1} \times F_f) + [(R_{a2} \times F_a) + (R_{b2} \times F_b) + (R_{c2} \times F_c) + (R_{d2} \times F_d) + (R_{e2} \times F_e) + (R_{f2} \times F_f) + [(R_{a3} \times F_a) + (R_{b3} \times F_b) + (R_{c3} \times F_c) + (R_{d3} \times F_d) + (R_{e3} \times F_e) + (R_{f3} \times F_f) + [(R_{a4} \times F_a) + (R_{b4} \times F_b) + (R_{c4} \times F_c) + (R_{d4} \times F_d) + (R_{e4} \times F_e) + (R_{f4} \times F_f) + [(R_{a5} \times F_a) + (R_{b5} \times F_b) + (R_{c5} \times F_c) + (R_{d5} \times F_d) + (R_{e5} \times F_e) + (R_{f5} \times F_f) + [(R_{a7} \times F_a) + (R_{b7} \times F_b) + (R_{c7} \times F_c) + (R_{d7} \times F_d) + (R_{e7} \times F_e) + (R_{f7} \times F_f)$$

where DN is the spectral reflectance of a pixel in the Landsat 7 band composite image, R_{ij} is the known DN or spectral reflectance or endmember values for coconut, road, laterite outcrops, construction, arecanut and cloud. The six bands of the Landsat scene were represented by the parameter i and each of the six end-members was represented by factor j. F_j was the fraction coefficient of the jth component within the pixel or the fractional cover for coconut, road, laterite outcrops, construction, arecanut and cloud.

Pure features in a mixed pixel are referred to as endmembers of that pixel. The selection of appropriate endmembers to input into a linear model is important. It can be achieved in two ways[10]: (i) From a spectral (field or laboratory) library; and (ii) From the purest pixels in the image.

Endmembers obtained through the first option are generally referred as 'known', while those from the second option are called as 'derived'. Derived endmembers have preference over the 'known' because they are collected under the same atmospheric conditions. It saves from the necessity to atmospherically correct the image. Also, it sets aside the possibility of ignoring a pure endmember in the scene[11]. The homogeneous field of having at least 3×3 pixel area centre point coordinate was registered with the help of GPS (GS5+ Leica system). The same was co-registered in the satellite imagery and endmember pixel DN value was extracted.

DN values were converted to satellite radiance values by utilizing the information provided in the ancillary data of the scene (Table 1) as described below[12]:

$$L_i = \mathrm{DN}_i \times G_i + B_i,$$

where the subscript denotes band, L_i at satellite radiance (mW cm^{-2} sr^{-1}), DN the eight-bit Landsat-7 ETM$^+$ image data, and G_i and B_i are band-specific gains and bias, both of which were obtained from the image metadata (Table 1).

SMA was done for DN and radiance values. The algorithm was implemented in Microsoft Visual C^{++}. Since the SMA program was implemented as an unconstrained version, with no constraints on the values of the fraction images, not all fractional values were between 0 and 100, but some values were below 0 or above 100. In the next

Table 1. Landsat-7 ETM$^+$ sensor details showing wavelength range, gain and bias

Landsat-7 ETM$^+$ band	Wavelength range (μm)	Gain (mW cm^{-2} sr^{-1} μm^{-1})	Bias (mW cm^{-2} sr^{-1})
Band–1	0.45–0.52	0.06024	–0.152
Band–2	0.52–0.60	0.11751	–0.284
Band–3	0.63–0.69	0.08057	–0.117
Band–4	0.76–0.90	0.08145	–0.151
Band–5	1.55–1.75	0.01211	–0.370
Band–7	2.08–2.35	0.00569	–0.015

step the fractional values of below 0 endmembers were eliminated and the SMA program was again implemented. The values above 100 were considered outside the range of the endmembers and were stretched to 100. Ideally, the algorithms that generate mixture maps constrain the individual material fractions to the range of 0.0 to 1.0 and the sum of the fractions for a single pixel totals to 1.0. The output fraction images were reclassified in IDRISI with five classes, i.e. < 20, 40, 40–60, 60–80% and above 80%. This scaling was chosen for three main reasons. First, it increased the interpretability of each fractional image, as used by the original SMA implementation from the University of Washington[13]. Secondly, fractions outside the above range are usually meaningless. Finally, for the economy of output data disk-storage space.

To assess the accuracy of final fraction maps and to evaluate the robustness of the method, the spatial clusters of delineated pixels corresponding to coconut signatures were selected from the population of a random subset of test sites and identified on the field by GPS (GS5+ Leica system). These test site proportion of coconut was then calculated in the polygon representing the field. For each test site, accumulation of the corresponding endmember fractions was calculated to indicate the area of the polygon as estimated by sub-pixel classification method. The accuracy of endmember fraction was estimated as the mean of the percentage absolute difference between actual and modelled estimates as described below.

$$\delta = \left(1 - \sum \frac{|\gamma - \sigma|}{\gamma} / n\right) 100,$$

where δ is the per cent correctness of sub pixel classification, γ is the actual area of a test site for the endmember, σ is the SMA modelled area of the test site for the endmember and n is the number of test sites.

Spectra for five different land-cover types existing in the study area were plotted for the image. These are the spectra obtained from the imagery (Figures 1 and 2). The endmember spectra for almost all the land-cover types showed similar pattern to each other. It indicates that arecanut had a low DN and radiance in visible and near infrared band 4. In the middle infrared band 5 and far infrared band 7, coconut had the lowest value. Better separability of different land-cover types was more pronounced at satellite radiance than DN value, particularly in the visible region of the spectrum.

In the image, water bodies were masked and the fraction image was developed using SMA based on DN and radiance values. Figure 3 is a fraction set for coconut LANDSAT-7 ETM$^+$ data. It indicates that 69% of the pixels had coconut in the instantaneous field of view (IFOV). The median of fraction of coconut in the study area was 0.42. Only two per cent of the pixels having coconut had land-cover fraction of more than 0.75 for coconut (Figure 4).

Accuracy assessment for each classified image was conducted based on the test data from GPS registered ground-truth points and fractional image. The error matrix was created for coconut cover type. The subpixel accuracy achieved for the coconut land-cover was 87% by using SMA of DN values, while it was 93% for SMA of radiance values.

The selection of endmembers is a critical component to successful application of mixture modelling. The first uses reflectance spectra measured in the field or laboratory. This method allows great control over the selection of endmember spectra, but requires that raw image data be correctly converted to reflectance, an often difficult task in remote sensing. It is also often difficult to obtain reference endmember spectra for all cover types. The second approach derives endmember spectra directly from the image by extracting reflectance from relatively 'pure' pixels from the field survey. Using image endmembers bypasses the need for ground measurements of cover-type reflectance, as well as the need for accurate, atmospherically correct images. In our study we used endmembers selected from the image.

Land-cover reflectance varies widely with changes in canopy structure and leaf chemistry[14] and variability for land area changes in mineralogy, organic matter content, and moisture[15]. In the study area almost similar pattern of spectral response for all the endmembers was observed with separability in the visible region of the spectrum.

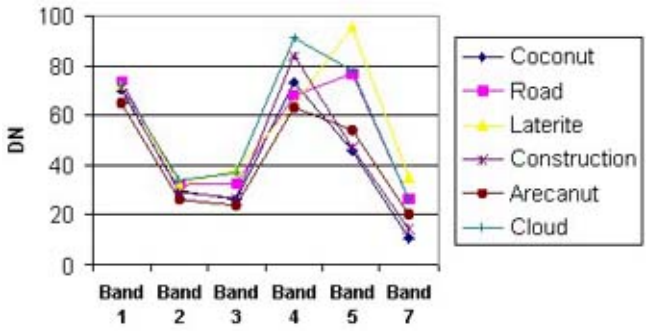

Figure 1. Endmember DN values of different LANDSAT-7 bands.

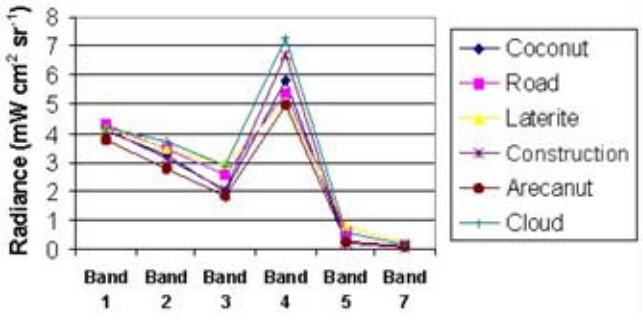

Figure 2. Endmember at satellite radiance of different LANDSAT-7 bands.

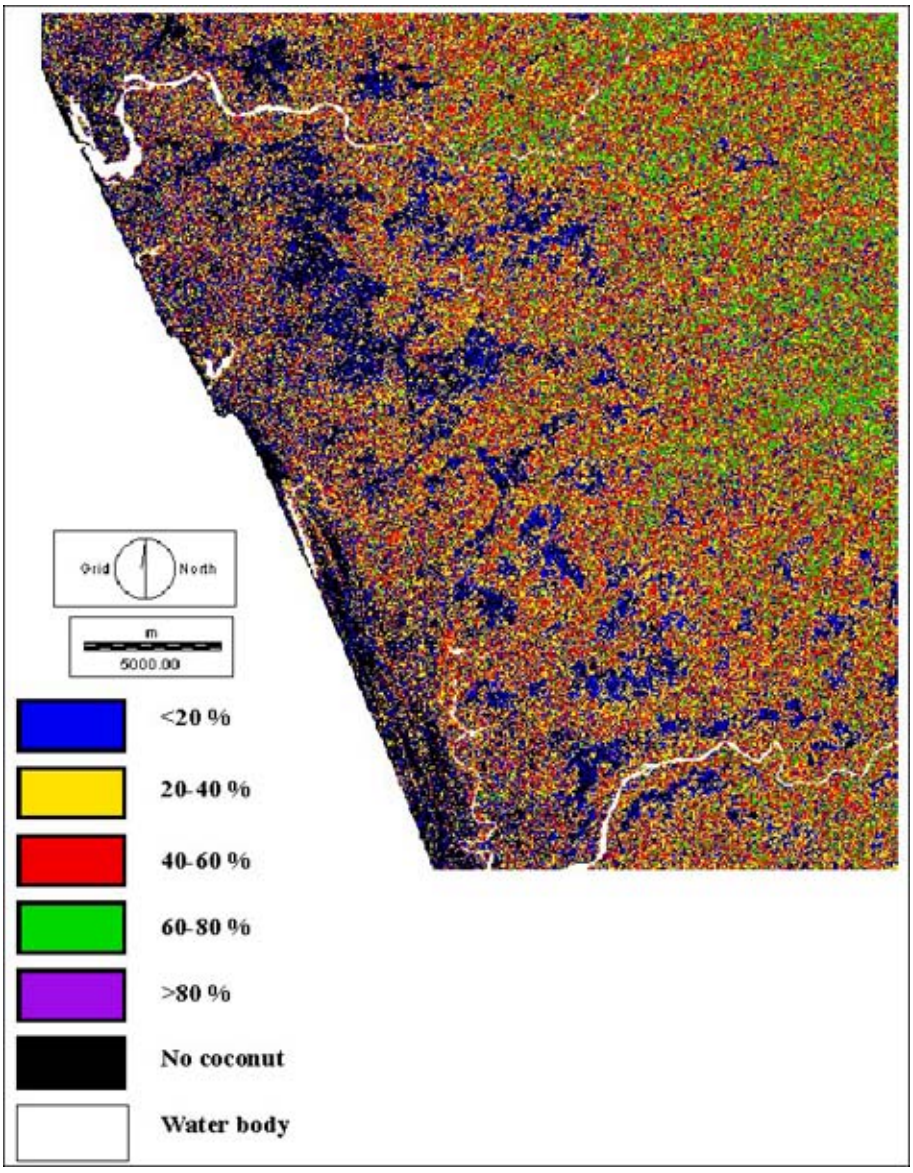

Figure 3. Fraction image of land-cover maps of coconut for toposheet part of Kasaragod district, Kerala.

Linear spectral unmixing was applied on the endmembers to complete the dataset of Landsat-7 ETM$^+$ image. To develop high-quality fraction images, relatively unimportant land-cover types like water (or shade) should be masked before the SMA procedure[16]. Masking of water bodies before SMA procedure was adopted in this study also. Unconstrained unmixing is chosen. It is preferred over constrained unmixing, as there is no use of artificially constraining the mixing for non negativity. It will just apply a linear correction after having unmixed the data. The advantage of unconstrained unmixing is that we can assess the results. If there are negative abundances for any of the endmembers then the unmixing does not make any physical sense. One reason for this may be the incorrect selection of endmembers. Hence, it is better to run unmixing iteratively to examine the abundance image and RMS error image. Ideally, the RMS image should not have high errors, and all of the abundance images are non-negative and sum to less than one. This iterative method is much more accurate than trying to artificially constrain the mixing, as in this way it is possible to detect the errors of the model[11].

Fraction image of endmember has been found valuable for identifying coconut land-cover type. A study[17] investigated selective logging with soil fraction images, which highlighted cleared landings where logs are stored before being transported to mills. An automated Monte Carlo spectral mixture was used in the model with Landsat-7 ETM imagery to detect landings, roads, skid trails and tree-fall gaps associated with selective logging in the eastern Amazon[18].

The cumulative frequency distribution for coconut land-cover fraction of 0.50 is 68%. Coconut is mostly cultivated as a small holder crop, the average size of a

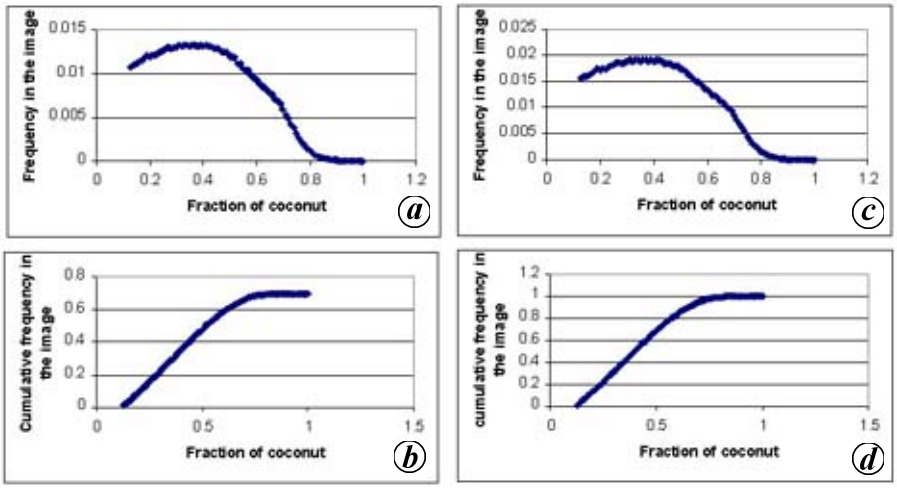

Figure 4. Frequency of coconut fractions in the pixel based on entire study area (***a*** and ***b***) and presence of coconut in the pixel (***c*** and ***d***).

holding being 0.22 ha. These small holders cultivate large number of crops to meet their diverse needs, such as food, fuel, timber, fodder and cash[19]. The canopy cover of coconut is about 75% in ideally spaced coconut gardens. In the study area the pure endmember for coconut land-cover is in low frequency. Light transmittance study at CPCRI, Kasaragod showed that 26.7% of the incident light is available for the under storey intercrop in the 40-year-old coconut garden[20].

Thus the SMA can be extrapolated to different dates of LANDSAT-7 images for change detection or for classification of land-cover types in a large area. Earlier studies have shown that the SMA is a promising approach for land-cover classification and change detection in the moist tropical regions[21–23]. Caution must be taken when the multitemporal LANDSAT data have different sun-elevation angles, especially in a rugged region like the present study area. In this case, accurate topographic correction using digital elevation model (DEM) data may be necessary.

Soil fertility, topography and land-use history influence the vegetation[24,25]. Vegetation stand structures, vegetation vigour and soil conditions affect the reflectance values captured by remote sensing sensors. Due to the complexity of biophysical environments on coconut, remote sensing signatures cannot effectively reflect the very small fraction of coconut in IFOV. This makes abundance estimation of coconut difficult in very small fractions, which could be the reason for not attaining 100% subpixel classification accuracy.

Earlier studies had demonstrated that spectral, spatial-based classifications were confirmed to provide better results than other per pixel classifiers[26–28]. However, due to the limitation of radiometric and spectral resolution, it is difficult to greatly improve the SMA classification accuracy for coconut land-cover. In terms of the availability of new sensors and data, optical and microwave data provide complementary information about land-cover and vegetation fragmentation. Besides overcoming the problem of cloud cover, use of radar data or integration of radar data with multispectral data is a promising way for future land-cover mapping[29–31].

In our study, SMA performed on radiance values gave better subpixel classification accuracy than SMA on DN values. Calibration of image data to radiance is not necessary for image classification with maximum likelihood or other per pixel classifiers using a single-data image. As long as the training data and image to be classified are on the same relative scale, calibration of image had little effect on classification accuracy[32]. However, the numerical seperability measure as a fraction of range and maximum value in the band among different endmembers is numerically high in radiance values (51.58% for DN value and 76.02% for radiance value in band 5).

An alternative to improve the extraction of earth surface feature information for vegetation classification in the study area is to use of state-of-the-art techniques for image processing and classification. ART–MMAP (Adaptive Resonance Theory – Mixture Mixture Analysis Model) based on neural network approach to subpixel classification estimated the fractions of land-cover with higher accuracy[33]. Independent component analysis aided linear spectral mixture analysis[34] and nonlinear spectral mixture model by genetic algorithm optimization technique are among the main trends to improve the subpixel classification accuracy.

The advantage of the fraction images extracted by this technique is that they contain different land-cover components within a pixel. This study demonstrates the possibility of using SMA as a subpixel technique to map coconut land-cover in the study area in Kasaragod district, Kerala. The results show considerable capability of

this technique to classify the main land-cover types. It is clear that this technique gives more accurate results in case of homogenous coconut land-cover. SMA could be used successfully to classify different vegetation covers in intensive agricultural areas. It is also to be noted that the method is easy to implement and has low computational cost.

1. Jasinski, M. F., Estimation of subpixel vegetation density of natural regions using satellite multispectral imagery. *IEEE Trans. Geosci. Remote Sensing*, 1996, **34**, 804–813.
2. DeFries, R. S., Townshend, J. R. G. and Hansen, M. C., Continuous fields of vegetation characteristics at the global scale at 1 km resolution. *J. Geophys. Res.*, 1999, **104**, 16911–16925.
3. Campbell, J. B., *Introduction to Remote Sensing*, The Guilford Press, New York, USA, 1996, 2nd edn.
4. Atkinson, P. M., Cutler, M. E. J. and Lewis, H., Mapping subpixel proportional cover with AVHRR imagery. *Int. J. Remote Sensing*, 1997, **18**, 917–935.
5. DeFries, R. S., Hansen, M. C. and Townshend, J. R. G., Global continuous fields of vegetation characteristics: A linear mixture model applied to multi-year 8 km AVHRR data. *Int. J. Remote Sensing*, 2000, **21**, 1389–1414.
6. Settle, J. and Drake, N. A., Linear mixing and the estimation of ground cover proportions. *Int. J. Remote Sensing*, 1993, **14**, 1159–1177.
7. Bateson, A. and Curtiss, B., A method for manual endmember selection and spectral unmixing. *Remote Sensing Environ.*, 1996, **55**, 229–243.
8. Foody, G. and Cox, D., Sub-pixel land cover composition estimation using a linear mixture model and fuzzy membership functions. *Int. J. Remote Sensing*, 1994, **15**, 619–631.
9. Huguenin, R. L., Karaska, M. A., Van Blaricom, D. and Jensen, J. R., Subpixel classification of bald cypress and tupelogum trees in Thematic Mapper imagery. *Photogramm. Eng. Remote Sensing*, 1997, **63**, 717–725.
10. Freek van der Meer, Image classification through spectral unmixing. In *Spatial Statistics for Remote Sensing*, Kluwer Academic Publishers, 1999, pp. 185–193.
11. Samia Ali, Use of spectral and temporal unmixing for crop identification using multi-spectral data. Ph D thesis, ITC, International Institute For Geo-Information Science and Earth Observation Enschede, The Netherlands, 2002, pp. 1–63.
12. Song, C., Cross-sensor calibration between Ikonos and Landsat ETM$^+$ for spectral mixture analysis. *IEEE Geosci. Remote Sensing Lett.*, 2004, **1**, 272–276.
13. Quarmby, N. A., Townshend, J. R. G., Settle, J. J., Milnes, M., Hindle, T. L. and Silleos, N., Linear mixture modelling applied to AVHRR data for crop area estimation. *Int. J. Remote Sensing*, 1992, **13**, 415–425.
14. Jacquemoud, S., Baret, F., Andrieu, B., Danson, F. M. and Jaggard, K., Extraction of vegetation biophysical parameters by inversion of the PROSPECT + SAIL models on sugar beet canopy reflectance data. Application to TM and AVIRIS sensors. *Remote Sensing Environ.*, 1995, **52**, 163–172.
15. Ben-Dor, E., Irons, J. R. and Epema, G. F., Soil reflectance. In *Remote Sensing for the Earth Sciences: Manual of Remote Sensing* (ed. Rencz, A. N.), Wiley & Sons, New York, 1999, pp. 111–188.
16. CSIRO, http://www.cmis.csiro.au/iap/RecentProjects/hyspec_eg.htm, 2003.
17. Souza, C. and Barreto, P., An alternative approach for detecting and monitoring selectively logged forests in the Amazon. *Int. J. Remote Sensing*, 2000, **21**, 173–179.
18. Asner, G. P., Keller, M., Pereira, R., Zweede, J. C. and Silva, J. N., Forest canopy damage and closure following selective logging in Amazonia: Integrating satellite and field studies. *Ecol. Appl.*, 2002.
19. Sairam, C. V., Arulraj, S. Joshi, G. V., Palaniswami, C. and Damodaran, V. K., Economics of palm based farming system. Central Plantation Crops Research Institute, Kasaragod, Kerala, 2004, p. 48.
20. CPCRI, Annual Report 2003–04. Central Plantation Crops Research Institute, Kasaragod, 2004, p. 35.
21. Adams, J. B., Sabol, D. E., Kapos, V., Filho, R. A., Roberts, D. A., Smith, M. O. and Gillespie, A. R., Classification of multispectral images based on fractions of endmembers: Application to land-cover change in the Brazilian Amazon. *Remote Sensing Environ.*, 1995, **52**, 137–154.
22. Roperts, D. A. *et al.*, Large area mapping of landcover change in Rondonia using decision tree classifiers. *J. Geophys. Res. D*, 2002, **107**, 8073.
23. Roberts, D. A., Batista, G. T., Pereira, J. L. G., Waller, E. K. and Nelson, B. W., Change identification using multitemporal spectral mixture analysis: Applications in eastern Amazonia. In *Remote Sensing Change Detection: Environmental Monitoring Methods and Applications* (eds Lunetta, R. S. and Elvidge, C. D.), Ann Arbor, MI: Ann Arbor Press, 1998, pp. 137–161.
24. Lu, D., Moran, E. and Mausel, P., Linking Amazonian secondary succession forest growth to soil properties. *Land Degrad. Dev.*, 2002, **13**, 331–343.
25. Moran, E. F., Brondýzio, E. S., Tucker, J. M., da Silva-Forsberg, M. C., McCracken, S. D. and Falesi, I., Effects of soil fertility and land use on forest succession in Amazonia. *For. Ecol. Manage.*, 2000, **139**, 93–108.
26. Brondizio, E. S., Moran, E. F., Mausel, P. and Wu, Y., Land cover in the Amazon estuary: Linking of the Thematic Mapper with botanical and historical data. *Photogramm. Eng. Remote Sensing*, 1996, **62**, 921–929.
27. Mausel, P., Wu, Y., Li, Y., Moran, E. F. and Brondizio, E. S., Spectral identification of succession stages following deforestation in the Amazon. *Geocarto Int.*, 1993, **8**, 61–72.
28. Moran, E. F., Brondizio, E. S. and Mausel, P., Secondary succession. *Res. Explor.*, 1994, **10**, 458–476.
29. Rignot, E., Salas, W. A. and Skole, D. L., Mapping deforestation and secondary growth in Rondônia, Brazil, using imaging radar and Thematic Mapper data. *Remote Sensing Environ.*, 1997, **59**, 167–179.
30. Saatchi, S. S., Soares, J. V. and Alves, D. S., Mapping deforestation and land use in Amazon rainforest by using SIR-C imagery. *Remote Sensing Environ.*, 1997, **59**, 191–202.
31. Yanasse, C. C. F., Sant'Anna, S. J. S., Frery, A. C., Renno, C. D., Soares, J. V. and Luckman, A. J., Exploratory study of the relationship between tropical forest regeneration stages and SIR-C L and C data. *Remote Sensing Environ.*, 1997, **59**, 180–190.
32. Kawata, Y., Ohtani, A., Kusaka, T. and Ueno, S., Classification accuracy for the MOS-1 MESSR data before and after the atmospheric correction. *IEEE Trans. Geosci. Remote Sensing*, 1990, **28**, 755–760.
33. Liu, W., Seto, K. C. Wu, E. Y., Gopal, S. and Woodcock, C. E., ART-MMAP: A neural network approach to subpixel classification. *IEEE Trans. Geosci. Remote Sensing*, 2004, **42**, 1976–1983.
34. Kosaka, N. and Kosugi, Y., ICA aided linear spectral mixture analysis of agricultural remote sensing images. In 4th International Symposium on Independent Component Analysis and Blind Signal Separation (ICA 2003), Nara, Japan, April 2003, pp. 221–226.

Received 18 February 2006; revised accepted 18 July 2006